Available online at www.sciencedirect.com
SCIENCE DIRECT®
Polymer 45 (2004) 1697–1706
polymer
www.elsevier.com/locate/polymer

Polyimide-silica nanocomposites: spectroscopic, morphological and mechanical investigations

Pellegrino Musto[a,*], Giuseppe Ragosta[a], Gennaro Scarinzi[a], Leno Mascia[b]

[a]*Institute of Chemistry and Technology of Polymers (ICTP), National Research Council of Italy, Via Campi Flegrei 34, Olivetti Building 70, 80078 Pozzuoli, NA, Italy*
[b]*Institute of Polymer Technology and Materials Engineering, University of Loughborough, Loughborough LE11 3TU, UK*

Received 26 March 2003; received in revised form 2 December 2003; accepted 8 December 2003

Abstract

Polyimide/silica hybrids were prepared by a sol–gel process and were evaluated in terms of curing behaviour, morphology and mechanical properties at different temperatures. The spectroscopic examinations showed that the presence of inorganic phase accelerates both the removal of the solvent and the concomitant imidization reaction. Two types of morphology for the silica phase were obtained by tailoring the composition of the precursor solution mixture. The mechanical properties were found to be strongly dependent on the system morphology. The largest increase in rigidity and strength properties were achieved when the two phases were co-continuous. Furthermore, these nanocomposites exhibited better mechanical properties also at high temperatures, thus extending the possible service temperature range of the polyimides.

Keywords: Nanocomposites; Polyimide; FTIR

1. Introduction

Polyimides are well known for their outstanding properties in terms of thermal-oxidative stability, mechanical properties, high glass transition temperature and good resistance to solvents [1–3]. For this reason they are widely utilized in electrical and electronic applications [4]. More recently, they have been used as polymeric components of hybrid organic–inorganic (O–I) systems via the sol–gel route [5–8]. O–I hybrid systems are an important class of new-generation materials which combine the desirable properties of a ceramic phase (heat resistance, retention of mechanical properties at high temperatures and low thermal expansion) and those of organic polymers (toughness, ductility and processability). Among the various approaches used to produce hybrid composites, the sol–gel route provides a unique and versatile method. It can be viewed as a two-step network forming process, the first step being the hydrolysis of a metal alkoxide and the second consisting of a polycondensation reaction [9,10]. Polyimides are particularly suitable for this type of process, since they can be produced from polyamic acid precursors, which are soluble in hygroscopic solvents and can, therefore, tolerate the addition of water necessary to accomplish the hydrolysis of the alkoxide. Moreover, since the condensation reaction for the conversion of a polyamic acid to the corresponding polyimide is an intramolecular process, it is not expected to be affected by the surrounding inorganic network.

In the present study polyimide/silica hybrid materials were prepared by the sol–gel route, and characterized in terms of their curing behaviour, morphology and mechanical properties. In previous studies it was established that the morphology of the polyimide/silica hybrid can be controlled by using a coupling agent such as γ-glycidyloxypropyltrimethoxysilane (GOTMS) [5,8]. Thus, conventional, micron sized particulate composites were produced in the absence of GOTMS and nano-structured, co-continuous nanocomposites were obtained by introducing the coupling agent in the precursor solution for the silica phase.

In comparison to previous studies [5,8,11,12], in the present work the investigated materials were characterized

* Corresponding author. Tel.: +39-081-8675202; fax: +39-081-8695230.
E-mail address: musto@irtemp.na.cnr.it (P. Musto).

0032-3861/$ - see front matter © 2003 Elsevier Ltd. All rights reserved.
doi:10.1016/j.polymer.2003.12.044

in detail by means of time-resolved FTIR spectroscopy. In particular, this technique was used to study the solvent-loss kinetics from the polyamic acid solution and the imidization reaction.

Furthermore, the mechanical properties were investigated not only at ambient temperature but over a range from 20 to 250 °C, demonstrating the superior performances of the nanocomposites with respect to those of the unmodified polyimide.

2. Experimental

2.1. Materials

The polyimide precursor used in this study was Pyre-ML RK 692 from I.S.T (Indian Orchard, MA), commercially available as a 12 wt% solution in a mixture of *N*-methyl-2-pyrrolidone (NMP) and xylene (weight ratio 80:20). The precursor was a polyamic acid formed by condensation of pyromellitic dianhydride (PMDA) and oxydianiline (ODA) having $\bar{M}_w = 1.0 \times 10^5$ and $\bar{M}_n = 4.6 \times 10^4$. High purity grades of tetraethoxysilane (TEOS) and γ-glycidyloxypropyltrimethoxysilane (GOTMS) were obtained from Aldrich (Milwaukee, WI). Distilled water was used to induce hydrolysis of the alkoxysilane components using a 32 wt% HCl solution as catalyst and ethanol as solvent.

2.2. Film preparation

The alkoxysilane solutions used for the production of the polymer/silica hybrid films were prepared from either pure TEOS or TEOS/GOTMS mixtures. In a typical formulation (N22) 3.46 g of TEOS, 0.86 g of EtOH, 1.20 g of GOTMS, 0.82 g of H_2O and 0.12 g of an aqueous HCl solution (2.0 wt%) were added sequentially in a glass vial. The mixture was magnetically stirred at room temperature (RT), until a clear solution was obtained. A slight heat evolution indicated the starting of an exothermic hydrolysis reaction and the alkoxysilane solution was allowed to mature at RT for about 10 min prior to being mixed with the polyamic acid solution. The precursor hybrid solution was subsequently obtained by adding dropwise the hydrolysed alkoxysilane solution to the polyamic acid solution, under continuous stirring for 10 min at RT.

The solutions were then used immediately for the production of 20–30 μm thick films. These were prepared by spreading the hybrid solution onto a glass plate with the aid of a Gardner knife. The cast films were allowed to dry first for 1 h at RT and then for 1 h at 80 °C at atmospheric pressure. Clear films were obtained for both pure polyimide and the nanocomposites containing the GOTMS coupling agent. Opaque films with a particulate morphology (microcomposites) were obtained in the absence of GOTMS. Finally, the samples were cured stepwise at 100, 150, 200, 250 and 300 °C for 1 h at each temperature. The cured films were peeled off from the glass substrate by immersing in distilled water at 80 °C. For FTIR spectroscopy measurements the films were cast onto KBr windows. A film thickness of about 5 μm was obtained by spreading the solution with a razor blade. The composition and codes of the polyimide/silica mixtures are detailed in Table 1.

2.3. Techniques

2.3.1. FTIR spectroscopy

Transmission FTIR spectra were obtained using a System 2000 spectrometer from Perkin–Elmer (Norwalk, CT). This instrument employs a Germanium/KBr beam splitter and a deuterated tryglycine sulfate (DTGS) detector. The instrumental parameters adopted for the spectral collection were as follows: resolution 4 cm^{-1}, optical path difference (OPD) velocity = 0.20 cm s^{-1}, spectral range 4000–400 cm^{-1}. A single data collection was performed for each spectrum (3601 data points), which in the selected instrumental conditions took 6 s to complete. It was found that, even with a single acquisition, the signal-to-noise ratio of the spectra (5000:1) was suitable for quantitative analysis. A dedicated software package for the acquisition of time-resolved infrared spectra was used to drive the FTIR spectrometer during the test (Timebase V. 1.1 from Perkin–Elmer).

The experiments at controlled heating rate and the isothermal kinetic measurements were carried out in an environmental chamber constructed in house by modifying the commercially available SPECAC 20100 cell. This unit was controlled by a Eurotherm PID temperature regulator mod. 2416, with an accuracy of ± 0.5 °C. All measurement were carried out under a continuous flux of N_2 (60 cm^3 min^{-1}).

Quantitative analysis was carried out by monitoring the height of different analytical peaks as a function of temperature or time. Normalization of the peaks' height to compensate for thickness changes was accomplished by ratioing against an internal reference band (an aromatic ring mode at 1498 cm^{-1}), which was found to be invariant with the chemical modifications occurring upon curing. In particular, the solvent content in the sample was evaluated from a NMP peak at 985 cm^{-1}, while the degree of imidization was monitored by the imide absorption at 1376 cm^{-1} (imide II mode). The latter peak was chosen among the various absorptions characteristic of the imide linkage because it is insensitive to orientational effects and does not overlap to anhydride components [13]. The imidization degree, i.d., is evaluated as:

$$\text{i.d.}(t) = \frac{\bar{A}_t(1376)}{\bar{A}_f(1376)} \quad (1)$$

where $\bar{A}_t(1376)$ is the normalized absorbance of the 1376 cm^{-1} band (i.e. $A_t(1376)/A_t(1498)$) at time t and $\bar{A}_f(1376)$ is the normalized absorbance of the same band

Table 1
Codes and compositions of the investigated materials

Code	TEOS (mmol)	GOTMS (mmol)	H_2O (mmol)	HCl (mmol)	C_2H_5OH (mmol)	PYRE-ML (g)	PI (wt%)	Silica (wt%)	Appearance[a]
PAA	–	–	–	–	–	3.50	100	–	C
M10	0.798	–	2.183	0.0031	0.896	3.50	90.3	9.7	O
M17	1.530	–	4.211	0.0061	1.728	3.47	82.7	17.3	O
M22	2.111	–	5.778	0.0083	2.370	3.49	77.8	22.2	O
M28	2.933	–	8.000	0.0116	3.283	3.49	71.6	28.4	O
N10	0.635	0.194	1.739	0.0025	0.715	3.50	90.3	9.7	C
N17	1.240	0.377	3.394	0.0049	1.391	3.51	82.7	17.3	C
N22	1.687	0.517	4.611	0.0067	1.898	3.50	77.8	22.2	C
N28	2.332	0.712	6.389	0.0092	2.609	3.49	71.6	28.4	C

[a] C, clear; O, opaque.

after full cure of the polyimide. It is worth noting that, although the quantitative analysis relies on a signal of the imide group, the relative conversion obtained therefrom, may be also related to the amic acid, i.e. it may indicate the amount of reacted polyamic acid groups with respect to their initial concentration. For this extension to be valid it is necessary, however, to assume that no side reactions take place, and cyclization is the sole process occurring. In the above hypothesis we may write:

$$\frac{\bar{A}_t(1376)}{\bar{A}_f(1376)} = \frac{C_t^{IM}}{C_f^{IM}} = \frac{C_i^{AMA} - C_t^{AMA}}{C_i^{AMA}} = \alpha_{AM} \quad (2)$$

where C_i represents the concentration of the specified group initially present in the system and the superscripts IM and AMA refer, respectively, to imide and amic acid groups.

The FTIR spectra of the polyimide and the hybrid films after thermal treatment up to 300 °C, do not show any trace of residual unreacted amic acid groups.

In an analogous fashion the amount of residual solvent in the sample can be calculated from the expression:

$$\%\text{solvent} = \frac{\bar{A}(985)}{\bar{A}_i(985)} 100 \quad (3)$$

where $\bar{A}_i(985)$ is the normalized absorbance of the NMP peak at 985 cm^{-1} in the film of the polyimide precursor at ambient temperature. The knowledge of the initial composition of the Pyre-ML solution allows one to establish the absolute concentration of NMP in the sample from Eq. (3), and to calculate the molar ratio amic acid/NMP, where amic acid is the repeating unit of the polyamic acid.

2.3.2. Mechanical tests

Small dumb-bell specimens with waist dimensions of 20 × 3.5 mm were used for tensile mechanical tests. The specimens were tested using an Instron instrument (mod. 4505), equipped with a temperature control chamber, at a cross-head speed of 1 mm min^{-1} and in a temperature range from ambient temperature to 250 °C. At least five specimens were tested at each temperature. Stress–strain curves were recorded from which the modulus, the stress and the elongation at fracture were evaluated.

2.3.3. Morphology

The fractured surfaces of films obtained after cooling in liquid nitrogen were examined by scanning electron microscopy (SEM). The apparatus used was a Philip SEM mod. XL20 and the fracture surfaces were coated with a gold–palladium layer by vacuum sputtering.

2.3.4. Dynamic mechanical measurements

Dynamic mechanical tests were carried out using a Polymer Laboratories DMTA apparatus model MK III. The tests were performed in tensile mode in a temperature range from 200 to 500 °C at a heating rate of 5 °C min^{-1} and at an oscillating frequency of 5 Hz.

3. Results and discussion

3.1. FTIR spectroscopy

3.1.1. Solvent loss investigations

In order to study the influence of the inorganic phase on the curing process of the polyamic acid (PAA), thin films (about 5 μm) of a polyimide precursor and of a typical composition of the nanocomposite system were subjected to the standard curing protocol. The reactions were followed by means of time-resolved FTIR spectroscopy. Numerous studies have appeared in the literature on the curing of PAA which used IR spectroscopy as the principal tool to characterize the mechanism and the kinetics of the process [13–18]. In fact, this technique is well suited for studying thin films and the functional groups involved in the reaction (carboxylic acids and amides) display intense, readily identified absorptions near 1700 and 1640 cm^{-1}, respectively. Also the imide groups formed are clearly discernible in the IR spectrum, giving rise to several characteristic absorptions at around 1780, 1730, 1365 and 724 cm^{-1}. Well resolved peaks can be equally identified for the poly(amic acid) solvent NMP, making it possible to study the rate of solvent evaporation during processing.

In Fig. 1 are reported the FTIR spectra of a film of the polyimide precursor collected at 25, 80 and 100 °C during a heating ramp to reach the temperature of an isothermal

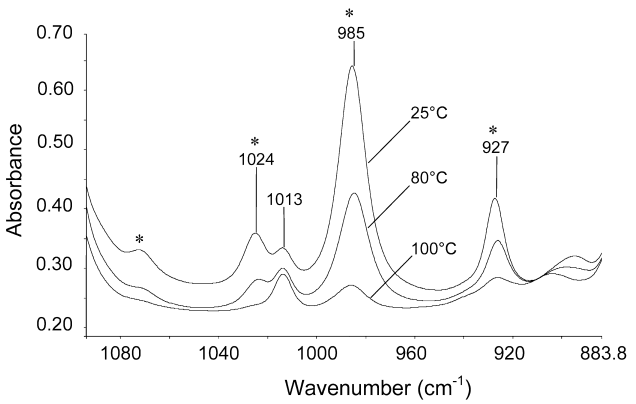

Fig. 1. Transmission FTIR spectrum in the wavenumber range 1080–880 cm^{-1} of the polyimide precursor (polyamic acid in a NMP/xylene mixture) at 25, 80 and 100 °C. The asterisks denote solvent peaks.

measurement at 120 °C. In the wavenumber interval displayed in Fig. 1 (1080–880 cm^{-1}) the spectrum of the N22 hybrid precursor (data not shown) is almost coincident with that of the polyamic acid solution. The NMP peaks at 985 and 927 cm^{-1} are well suited for quantitative analysis. After normalizing for thickness (by taking the ratio of the aromatic absorption at 1498 cm^{-1}), this ratio may be conveniently used to determine the amount of residual solvent in the films. The solvent content, expressed as percent by weight with respect to the amount initially present in the sample, is reported in Fig. 2 as a function of temperature for the plain polyamic acid (curve A) and for the N22 nanocomposite precursor (curve B). It is noted that up to 50 °C the amount of NMP evaporated from the polyamic acid film is negligible. Evaporation starts at temperatures slightly above 60 °C and can be considered to be complete at 100 °C. At this temperature, however, the residual NMP solvent is not zero, but reaches a plateau value corresponding to 6.9 wt%, which remains nearly constant by further heating the sample up to 120 °C. The behaviour just described is in agreement with previous observations [18–20]. In order to explain this effect,

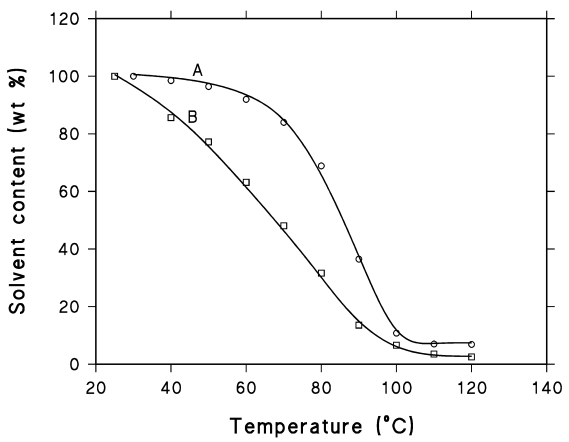

Fig. 2. Percent of residual NMP in the sample as a function of temperature for (A) the polyimide precursor; (B) the N22 nanocomposite.

Brekner and Feger [19,20] have suggested that the PAA repeat unit forms two well-defined complexes with NMP, whose stoichiometry corresponds to molar ratios 1:4 and 1:2 repeat-unit/NMP. The complex at molar ratio 1:2 is considerably more stable than the one at ratio 1:4. The activation energies for decomplexation are 110 kJ mol^{-1} for the 1:2 and 50 kJ mol^{-1} for the 1:4 complex. The molecular interactions involved in the complex formation are believed to be of the hydrogen-bonding type. In particular, the diamic acid moiety displays four functional groups able to form hydrogen bonds with NMP. The acid groups being stronger proton donors than the amide groups, gives rise to the formation of two complexes exhibiting different thermal stabilities [19,20].

The residual solvent present at high temperature in the polyimide film is likely to result from the complex at 1:2 molar ratio. From quantitative estimates of residual solvent, it is possible to evaluate the molar ratio between the amic acid units and complexed NMP in the 100–120 °C range. This gives a value of 1.81, which is very close to the value expected from stoichiometry (i.e. 2.0).

A completely different behaviour is observed with respect to these complexes in the N22 nanocomposite. In this case the solvent-loss starts at ambient temperature, and is considerably faster than for the polyamic acid. Although above 100 °C the residual amount of NMP in the N22 system is still not zero, it is more than three times lower than the value found for the polyamic acid (i.e. 2.13 wt% against 6.90 wt%). The observed enhancement in the rate of solvent removal from the PAA film brought about by the inorganic phase has relevant technological implications in that it can make the processing easier, particularly in the case of composite manufacturing.

The lower amount of residual solvent present in the nanocomposite at above 100 °C as compared to the control system may be explained by the reduced stability of the 1:2 complex. A possible reason for this is that the silica phase contains large amount of –OH groups which effectively compete with NMP in forming hydrogen-bonding interactions with the PAA units.

The hypothesis for the destabilization of the 1:2 complex is supported by the desorption kinetics of residual NMP from the two systems under isothermal curing at 120 °C. These data are compared in Fig. 3, which shows that for the pure polyimide precursor (curve A) the solvent desorption is rather fast in the early stages (up to about 200 min) and is followed by a slower steady-state regime. A detectable amount of residual solvent (1.0%) is still present in the sample, however, even after 1200 min. For the nanocomposite system (curve B), on the other hand, the lower amount of NMP initially present is lost completely in about 200 min. This implies that, while for the pure polyamic acid system most of the imidization reaction takes place in the presence of NMP, the same is not true for the imidization of polyamic acid in the nanocomposite.

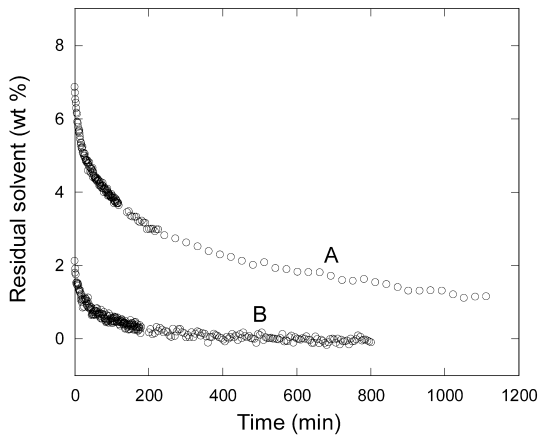

Fig. 3. Percent of residual solvent as a function of time during the isothermal imidization process at 120 °C. Curve A: the polyimide precursor; Curve B: the N22 nanocomposite.

3.1.2. Imidization kinetics

The kinetics of thermal imidization was evaluated spectroscopically by considering the evolution of the imide band at 1376 cm^{-1} (see Section 2 for details on quantitative analysis). The spectra in the wavenumber range 1480–1280 cm^{-1}, collected at different times during the isothermal curing at 120 °C for the polyimide precursor are shown in Fig. 4. In Fig. 5 is shown the degree of imidization for three different systems estimated from the spectroscopic data. In particular, curve A refers to the N22 nanocomposite, curve B is for the pure polyimide precursor and curve C is relative to a PAA film from which the NMP solvent was completely removed before curing, according to a procedure described in Ref. [21].

Although a considerable number of studies dealing with the curing kinetics of PAA films has been reported in the literature, the interpretation of the experimental data is still controversial [21–25]. While the cyclization of PAA into polyimide should be regarded as a first-order reaction in terms of amic acid concentration, since it involves two

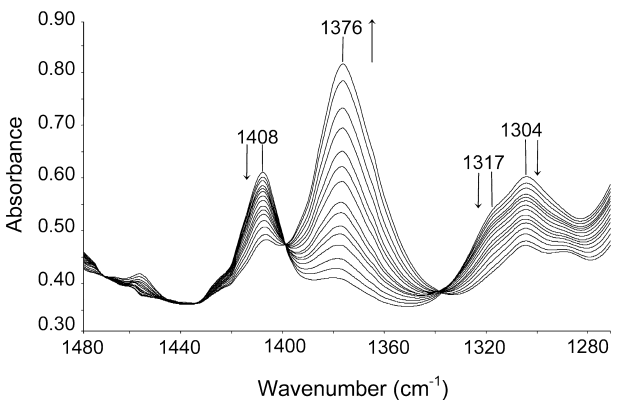

Fig. 4. Transmission FTIR spectra in the wavenumber range 1480–1280 cm^{-1} collected at various times during the isothermal imidization of the polyimide precursor at 120 °C.

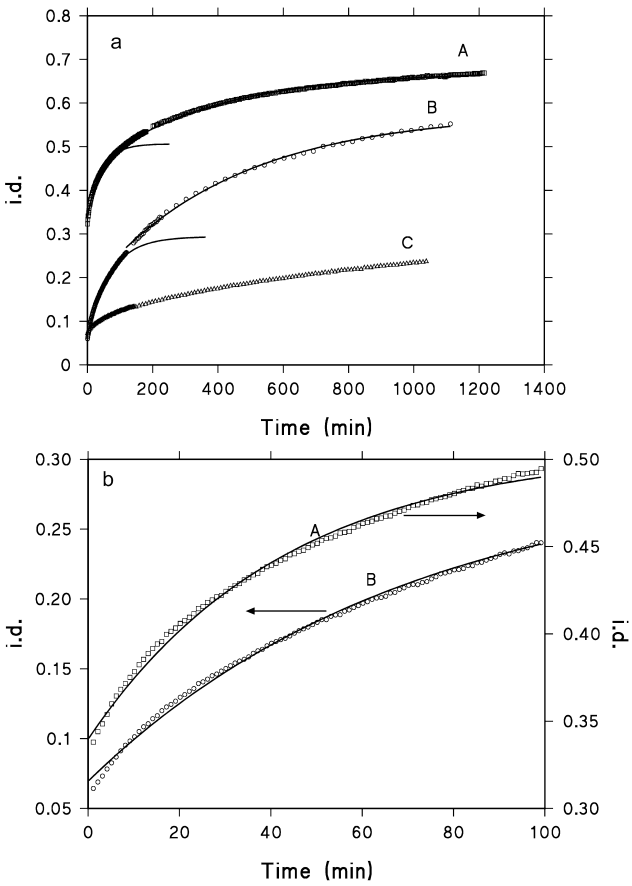

Fig. 5. Imidization degree (i.d.) as a function of time for the isothermal reaction at 120 °C. Curve A: N22 nanocomposite; Curve B: the polyimide precursor; Curve C: the polyimide precursor from which the solvent had been completely eliminated prior to curing. The symbols indicate the experimental data, while the continuous lines represent the simulations of the first order kinetic model. (a) Displays the whole time range investigated, while (b) shows the first regime lasting from 0 to 100 min.

functional groups belonging to the same amic acid fragment [22,23,25], numerous kinetic investigations have pointed out that this cannot be the case for the entire conversion range. Imidization takes place in two stages, a fast initial step followed by a second slower process. Some authors, however, still consider this a first order process with two rate constants. Others have pointed out that the reaction rate is constant only in the initial stage and decreases continuously to almost zero long before the complete conversion of the reactants. Such a process has been called kinetic interruption. By increasing the imidization temperature, the contribution due to the first stage increases [22,24,25].

For the kinetic analysis of the imidization reaction as a first-order model with residuals, the following rate equation can be used:

$$C = Ae^{-kt} + C_f \tag{4}$$

where A is a pre-exponential factor, k is the rate constant and C_f is the residual concentration of amide groups at time

$t \rightarrow \infty$. From the initial condition $C = C_0$ at $t = 0$, it follows that $A = C_0 - C_f$, i.e. the concentration of amide groups transformed into imide groups at $t \rightarrow \infty$.

Defining the relative conversion α as:

$$\alpha = \frac{C_0 - C}{C_0} = 1 - \frac{C}{C_0} \tag{5}$$

it follows that:

$$\alpha = \alpha_f(1 - e^{-kt}) \tag{6}$$

However, the relative conversion obtained from the spectroscopic data refer to the total concentration of amide groups initially present into the system, C_i (see Eq. (2)), rather than to C_0 (the concentration at zero time in the isothermal kinetic measurement) and C_i is significantly higher than C_0. To account for this discrepancy, the spectroscopic conversion, α' can be defined as:

$$\alpha' = \frac{C_i - C}{C_i} = 1 - \frac{C}{C_i} \tag{7}$$

and can be transformed into the kinetic conversion α, as follows:

$$\alpha = (\alpha' - \alpha'_0)\frac{C_i}{C_0} \tag{8}$$

where α'_0 is the spectroscopic conversion at time zero (i.e. $(C_i - C_0)/C_i$) and C_i/C_0 is given by:

$$\frac{C_i}{C_0} = \frac{1}{1 - \dfrac{\bar{A}_0(1376)}{\bar{A}_f(1376)}} \tag{9}$$

The kinetic data for the imidization of the pure polyamic acid shown in Fig. 5 (curve B) are in general agreement with other published results. In particular, it is found that not only the initial step but also the second regime can be adequately described as first order processes. The kinetic constants for these are collectively reported in Table 2. It is also worth to note that partial imidization (i.d. = 0.06) takes place during the heating ramp before reaching the isothermal temperature. For this reason the conversion curve does not start from the origin.

Several explanations have been put forward to account for the decrease of the cyclization rate at higher conversion and for the characteristic two-stage behaviour of the polyimide. The principal arguments are:

(i) In PAA the amic acid groups are in two non-equivalent kinetic states, differing in their conformation. One state is activated for cyclization while the other is not. The activated state rapidly cyclize during the first stage, while the remaining inactive groups react in the second stage [22,26].

(ii) The imidization reaction is enhanced by the presence of solvent. Therefore, the decrease in reaction rate is due to the gradual loss of residual solvent from the system [23,27].

(iii) As the cyclization proceeds, the T_g of the system increases, so that the polymer undergoes a rubber-to-glass transition. Since the transition from a unfavourable to a favourable conformation of the amic acid groups requires a rotation around a bond of the polymer chain, a decrease of the overall molecular mobility will reduce the rate of formation of active sites and hence the imidization rate [26–29].

Table 2
Parameters obtained from the kinetic analysis of the imidization reaction

Code		k_i (min^{-1})	$\frac{C_i - C_0}{C_i}$	$\frac{C_i - C_f}{C_i}$	R^2
PAA	First regime	0.015	0.06	0.24	0.997
	Second regime	0.0023	–	0.58	0.999
N22	First regime	0.023	0.33	0.51	0.997
	Second regime	0.0028	–	0.67	0.999

More recent models proposed in the literature try to reconcile the three effects but it is difficult to asses their relative importance [22,25].

For the ongoing discussion, particularly relevant is the interplay between imidization kinetics and solvent loss, in so far as the nanocomposite formulation was found to behave very differently in this respect, when compared to the pure polyamic acid. The data shown in Fig. 5, curve C, relative to a PAA film from which all NMP had been eliminated prior to curing, confirm the fundamental role of residual solvent in the cure kinetics of polyimides. In fact, a drastic reduction of the imidization rate is observed in comparison to the control system (compare curves C and B). A fast initial imidization stage can still be distinguished and again the reaction starts below 120 °C, suggesting that a certain amount of amic acid groups are present as active species. However, their concentration is very low in comparison to the solvent containing system, as demonstrated by the shorter duration of the initial stage and the lower conversion attained at the end of this regime. As the active groups are fully consumed, the reaction rate drops dramatically; in fact, in the absence of solvent which acts a an efficient plasticizer, the T_g of the material is high and the required conformational transition is strongly hindered.

The kinetic behaviour of the nanocomposite precursor resembles that of the pure polyamic acid in presence of solvent, in that it can be adequately described by two first-order regimes. The second of which has a rate constant considerably lower than the first. However, in the nanocomposite system the first stage is significantly faster than for the pure polyamic acid in solution (see the kinetic parameters collected in Table 2) and the imidization reaches a more advanced stage during the heating ramp from room temperature to 120 °C. The initial conversion of amic acid groups is 0.33 for the nanocomposite system and only 0.06 for the polyamic acid solution. As a consequence of these two effects the final conversion of amic acid is higher in the

nanocomposite than in the pure polyimide (0.67 against 0.58). The second stage of imidization in the two systems, however, is characterized by a comparable rate constant.

The kinetic behaviour for the nanocomposite precursor seems to be conflicting with the solvent effect in pure polyamic acid in so far as the residual solvent is much lower. There has to be, therefore, a component of the nanocomposite formulation, which plays the role of NMP in facilitating the conversion of inactive groups into active ones. As this effect cannot arise from higher molecular mobility of the PAA chains, a possible explanation for the catalytic activity of the inorganic phase with respect to imidization is that the silica domains, bearing a large amount of hydroxyl groups along the outer surface, may form strong molecular interactions of hydrogen bonding type with the amic acid groups of PAA. In doing so, the PAA chains may be forced to assume a planar conformation more favourable for cyclization. This effect has already been invoked in previous work to explain the different behaviour of PAA cured between two layers of silica and between two plates of a low-polarity polymer substrate (PEEK) [11]. Work is in progress to further substantiate this hypothesis by spectroscopic means.

3.2. Properties of the polyimide/silica hybrids

3.2.1. Mechanical properties and morphology

Typical tensile stress–strain curves for the investigated nanocomposite systems and for the parent polyimide are shown in Fig. 6. The polyimide sample (curve A) exhibits a gradual transition from elastic to plastic behaviour without a well-defined yielding point. A similar behaviour is observed for the polyimide/silica samples (curves B, C, D and E). For the latter, however, the presence of the inorganic phase reduces the extent of plastic flow of the polyimide phase and consequently, fracture takes place at progressively lower strains with increasing silica content.

The properties derived from the stress–strain diagrams

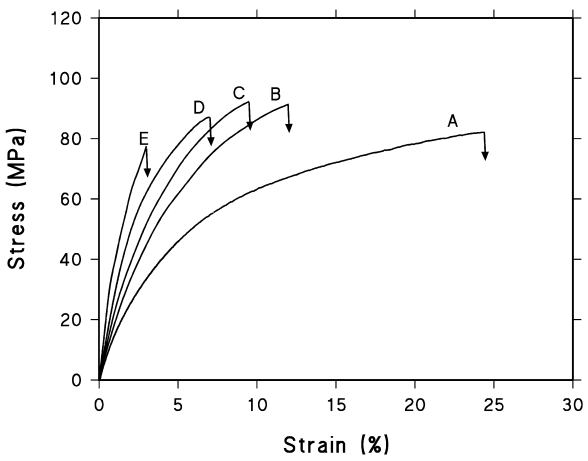

Fig. 6. Typical stress–strain curves of polyimide/silica hybrids: Curve A: plain polyimide; Curve B: N10 nanocomposite; Curve C: N17 nanocomposite; Curve D: N22 nanocomposite; Curve E: N28 nanocomposite.

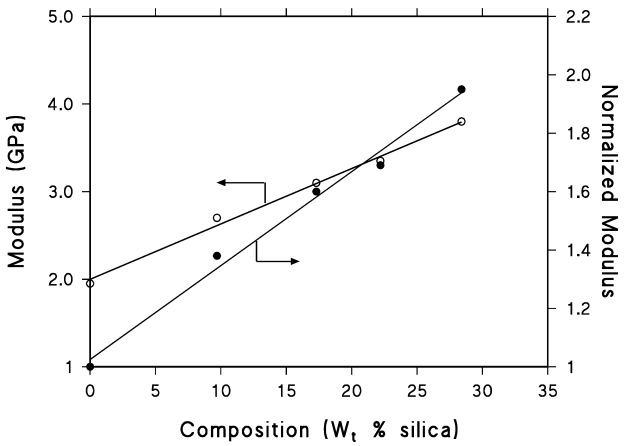

Fig. 7. Elastic modulus (○) and normalized elastic modulus (●) for the nanocomposite system as a function of the silica content.

in Fig. 6 are reported in Figs. 7 and 8. The modulus is found to increase linearly with increasing the concentration of the inorganic phase (Fig. 7). In the same figure, the data for the normalized modulus, (modulus enhancement factor) calculated as the ratio of the modulus of the nanocomposite to that of the polyimide reaches the value of 2 (i.e. 100% increase) at a silica content of 28.4%.

The plot of the tensile strength as a function of the silica concentration (Fig. 8) shows a gradual increase of the tensile strength up to a concentration of silica around 20 wt%, followed by a slight reduction at higher concentrations. The elongation at break, displayed in the same figure, exhibits a monotonic decrease. This suggests that the failure process is controlled mainly by structural modifications occurring within the polyimide matrix, rather than being determined by failure within the silica phase.

In Fig. 9 are shown the mechanical properties expressed in terms of tensile strength and elongation at break, for the same hybrid compositions obtained without the use of the compatibilizing agent (GOTMS). One notes that the tensile strength does not show the initial increase observed for the compatibilized systems, but decreases gradually over the

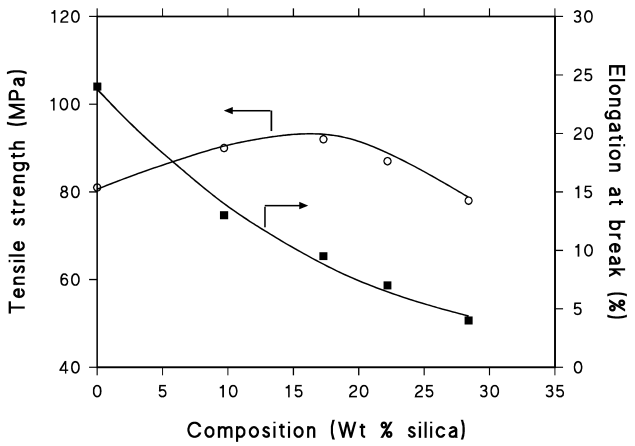

Fig. 8. Tensile strength (○) and elongation at break (■) for the nanocomposite system as a function of the silica content.

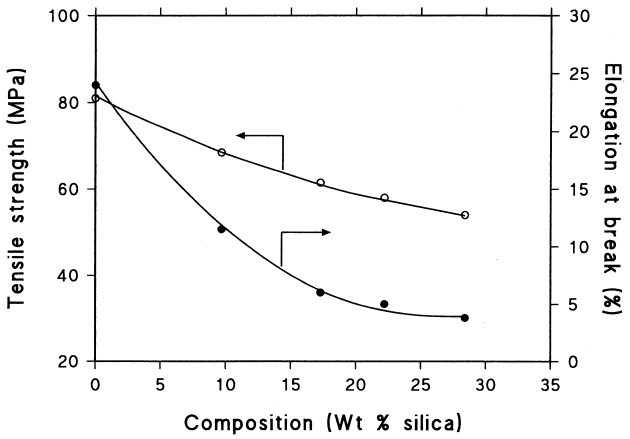

Fig. 9. Tensile strength (○) and elongation at break (●) for the microcomposite system as a function of the silica content.

whole composition range. The elongation at break displays a behaviour very close to that of the nanocomposite formulations.

It is known that in polymeric composites the external stress is transferred from the continuous polymeric matrix to the discontinuous reinforcing phase [30,31]. Thus, the ultimate properties of composite materials are dependent on the extent of bonding between the two phases, the surface area of the dispersed phase and the geometry of the reinforcing phase. In Fig. 10 are shown the scanning electron micrographs of polyimide/silica mixtures obtained with and without the addition of GOTMS. These micrographs show clearly the effect of GOTMS, which brings about a morphological transition from a dispersed-particle phase structure (Fig. 10(A)), in the absence of GOTMS to a fine interconnected or co-continuous phases morphology (Fig. 10(B)), with the use of GOTMS. For the compatibilized system the size of the interconnected silica domains ranges from 40 to 100 nm, while for the non-compatibilized system, the average diameter of the silica particles varies from 1 to 2 μm. The micrograph of Fig. 10(A) also reveals that the silica particles are very smooth and completely debonded from the surrounding polyimide matrix, indicating a very poor interfacial adhesion between the two phases.

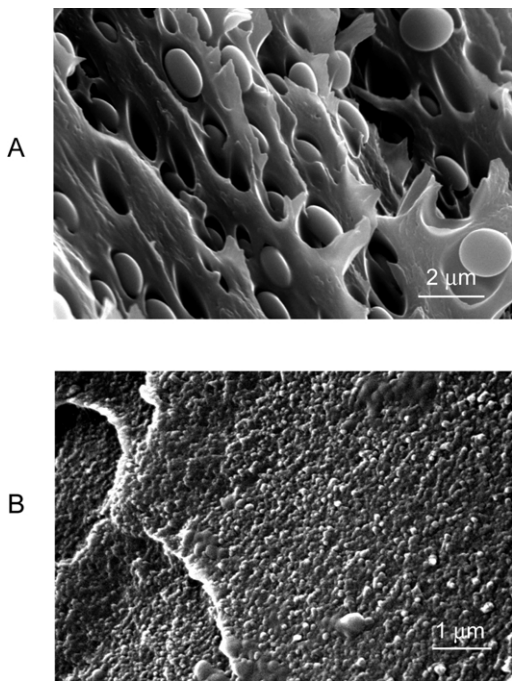

Fig. 10. SEM micrographs for the M22 microcomposite (A) and for the N22 nanocomposite (B).

On the basis of these morphological observations, it is evident that the reduction in ultimate properties observed for non-compatibilized systems can be attributed to weak interactions between the phases, which allow the silica particles to act as stress-concentration defects, rather than as effective reinforcing fillers. On the contrary, for compatibilized systems, the increased tensile strength is the result of both a better interfacial adhesion and the formation of co-continuous morphologies, which improve the efficiency of stress transfer mechanisms between the two components. In spite of the enhanced adhesion, the elongation at break decreases since the interconnected silica phase hinder the plastic flow of the polyimide phase preventing large deformations to occur prior to fracture.

The mechanical behaviour of compatibilized systems was also studied over the temperature range 20–250 °C. In Fig. 11 the variation of modulus with temperature for a mixture containing 22.3 wt% of silica is compared with that of the non-reinforced polyimide. A linear decrease of modulus with temperature is observed for both materials; a similar trend is found for the tensile strength (Fig. 12). The elongation at break, reported in Fig. 13, increases considerably with temperature for the case of polyimide, while only a slight increase is observed for the polyimide/silica hybrids. This effect reflects the more elastic character of the nanocomposite with respect to the plain polyimide.

Although the decrease in modulus and strength with temperature as well as the increase of strain at break are to be expected, the relevant findings from the above analysis

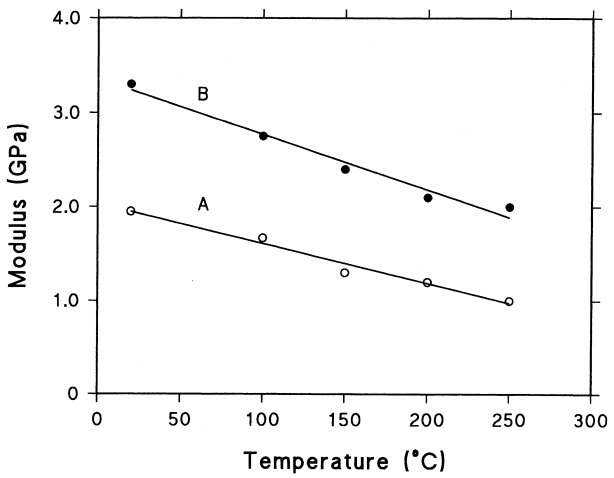

Fig. 11. Elastic modulus as a function of temperature for the plain polyimide (Curve A) and for the N22 nanocomposite (Curve B).

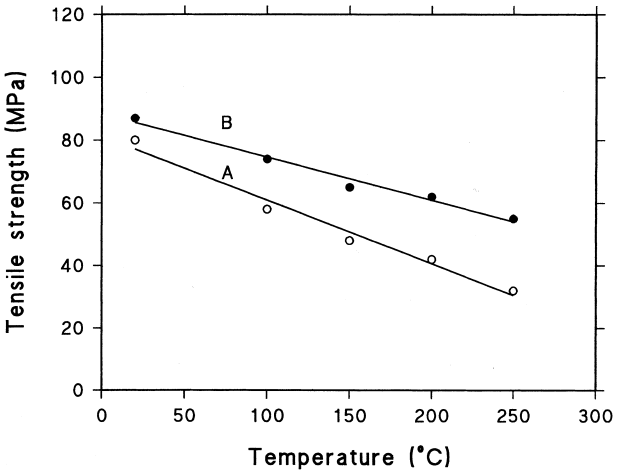

Fig. 12. Tensile strength as a function of temperature for the plain polyimide (Curve A) and for the N22 nanocomposite (Curve B).

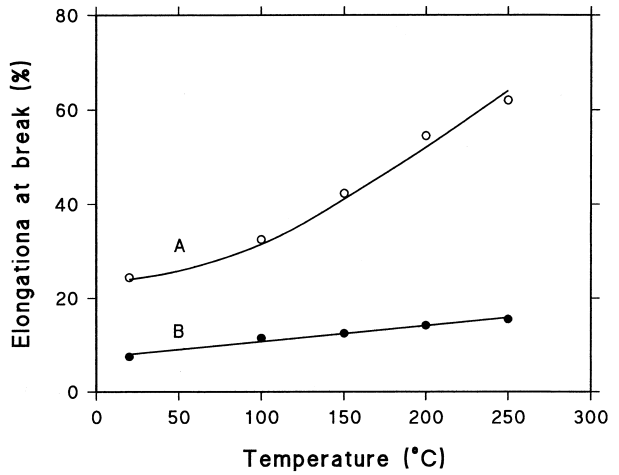

Fig. 13. Elongation at break as a function of temperature for the plain polyimide (Curve A) and for the N22 nanocomposite (Curve B).

are that at 250 °C, which is the limiting temperature for the continuous use of polyimides, the values of modulus and strength of the nanocomposites examined are very close to those of the base polyimide at ambient temperature. Thus, properly formulated nanocomposites would make it possible to extend considerably the maximum temperature at which these systems can be reliably employed relative to polyimides.

3.2.2. Dynamic-mechanical measurements

Fig. 14 shows the dynamic-mechanical spectra expressed in terms of tanδ for two polyimide/silica formulations (M28 and N28) and for the neat polyimide. All samples exhibit a principal relaxation peak, corresponding to the T_g, that for the two hybrid systems occurs at a temperature about 20 °C higher than that of the control material. Fig. 14 also shows that, for the polyimide/silica systems, there is a considerable reduction in the height of the tanδ peaks with respect to the

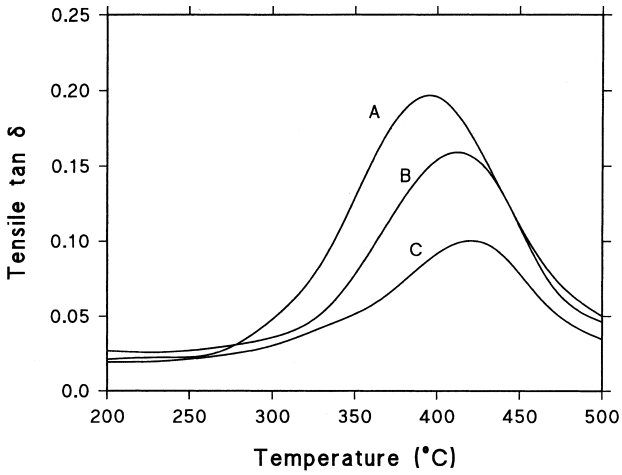

Fig. 14. Dynamic-mechanical spectra in terms of tanδ as a function of temperature. Curve A: plain polyimide; Curve B: M22 microcomposite; Curve C: N22 nanocomposite.

pure polyimide, indicating a decrease of the viscous response of the visco-elastic material [11]. This is clearly related to the presence of the fully elastic inorganic phase, but a further relevant observation is the enhancement of the effect in the nanocomposite system. Evidently, it reflects an improved phase interconnection and a better adhesion between the phases, which is achieved by the compatibilizing action of the GOTMS coupling agent.

4. Conclusions

A number of polyimide/silica hybrid systems have been prepared and characterized with respect to their curing behaviour, morphology and mechanical performances. A sol–gel type of process has been employed to produce nanocomposite structures or more conventional two-phase composites. A time-resolved spectroscopic analysis has pointed out that the presence of silica precursor within the pre-polymer solution greatly facilitates solvent removal from the film surface. At the same time, an inorganic phase is found to considerably accelerate the imidization of the polyamic acid.

In terms of mechanical properties, it is found that a co-continuous phase morphology with high adhesion between the phases brings about a general improvement of most mechanical parameters with respect to both the plain polyimide and hybrid systems where the inorganic phase forms discrete, micron sized domains with no adhesion to the polymer matrix. A further relevant conclusion is that both the modulus and the tensile strength of the nanocomposite systems display at 250 °C the same values exhibited by the plain polyimide at ambient temperature, which could in principle allow to extend the useful temperature range of the polyimide.

References

[1] Gosh MK, Mittal KL. Polyimides; fundamentals and applications. New York: Marcel Dekker; 1996.
[2] Feger C. Polyimides: trends in materials and applications. New York: Society of Plastic Engineers; 1996.
[3] Bessonov MI, Zubkov VA. Polyamic acids and polyimides: synthesis, transformation and structure. Boca Raton: CRC Press; 1993.
[4] Thompson LF, Willson CG, Tagawa S. Polymers for microelectronics: resists and dielectrics. ACS Symposium Series 537, Washington, DC: ACS; 1994.
[5] Mascia L. Trends Polym Sci 1995;3:61.
[6] Morikawa A, Iyoku Y, Kakimoto M, Imal Y. Polym J 1992;24:107.
[7] Nandi M, Conklin JA, Salvati Jr. L, Sen A. Chem Mater 1991;3:201.
[8] Kioul A, Mascia L. J Non-Cryst Solids 1994;175:169.
[9] Strawbridge I. In: Paul A, editor. Chemistry of glasses. London: Chapman and Hall; 1990.
[10] Huang H, Glaser RH, Wilkes GL. In: Zeldin M, Winne KJ, Allcock HR, editors. Inorganic and organometallic polymers. ACS Symposium Series 360, Washington, DC: ACS; 1987.
[11] Mascia L, Kioul A. Polymer 1995;3:3649.
[12] Mascia L, Kioul A. J Mater Sci Lett 1994;13:641.
[13] Pride CA. J Polym Sci, Polym Chem Ed 1989;27:711.
[14] Ginsberg R, Susko JR. In: Mittal K, editor. Polyimides, synthesis, characterization and applications. New York: Plenum Press; 1984. p. 237.
[15] Kumar D. J Polym Sci, Polym Chem Ed 1981;19:795.
[16] Snider RW, Thompson B, Bartges B, Czerniawski D, Painter PC. Macromolecules 1989;22:4166.
[17] Hsu TC, Liu ZL. J Appl Polym Sci 1992;46:1821.
[18] Shin TJ, Ree M. Macromol Chem Phys 2002;203:791.
[19] Brekner MJ, Feger C. J Polym Sci, Polym Chem Ed 1987;25:2005.
[20] Brekner MJ, Feger C. J Polym Sci, Polym Chem Ed 1987;25:2479.
[21] Numata S, Fujisaki K, Kinjo N. In: Mittal K, editor. Polyimides, synthesis, characterization and applications, New York: Plenum Press; 1984. p. 259.
[22] Laius LA, Tsapovetsky MI. In: Mittal K, editor. Polyimides, synthesis, characterization and applications. New York: Plenum Press; 1984. p. 311.
[23] Frayer PD. In: Mittal K, editor. Polyimides, synthesis, characterization and applications. New York: Plenum Press; 1984. p. 273.
[24] Pyun E, Mathiesen RJ, Sung CS. Macromolecules 1989;22:1174.
[25] Johnson C, Wunder SL. J Polym Sci, Polym Phys Ed 1993;31:677.
[26] Laius LA, Bessonov MI, Kallistova EV, Androva NA, Florinsky FS. Vysokomol Soedin 1967;9A:2185.
[27] Gillham JK, Gillham HC. Polym Engng Sci 1973;13:447.
[28] Laius LA, Bessonov MI, Florinsky FS. Polym Sci USSR 1971;13:2257.
[29] Koton MM. Polym Sci USSR 1971;13:1513.
[30] Clegg DW, Collier AA. Mechanical properties of reinforced thermoplastics. London: Elsevier; 1986.
[31] Hornsby PR, Hinrichsen E, Tarverdi K. J Mater Sci 1997;32:443.